

Linear Classifiers in Mixed Constant Curvature Spaces

Puoya Tabaghi¹ Eli Chien¹ Chao Pan¹ Olgica Milenković¹

Abstract

Embedding methods for mixed-curvature spaces are powerful techniques for low-distortion and low-dimensional representation of complex data structures. Nevertheless, little is known regarding downstream learning and optimization in the embedding space. Here, we address for the first time the problem of linear classification in a product space form — a mix of Euclidean, spherical, and hyperbolic spaces with different dimensions. First, we revisit the definition of a linear classifier on a Riemannian manifold by using geodesics and Riemannian metrics which generalize the notions of straight lines and inner products in vector spaces, respectively. Second, we prove that linear classifiers in d -dimensional constant curvature spaces can shatter exactly $d+1$ points: Hence, Euclidean, hyperbolic and spherical classifiers have the same expressive power. Third, we formalize linear classifiers in product space forms, describe a novel perceptron classification algorithm, and establish rigorous convergence results. We support our theoretical findings with simulation results on several datasets, including synthetic data, MNIST and Omniglot. Our results reveal that learning methods applied to small-dimensional embeddings in product space forms significantly outperform their algorithmic counterparts in Euclidean spaces.

1. Introduction

Machine learning methods in Euclidean spaces have been the focus of intense studies due to the fact that many practical datasets inherently lie in such spaces or are easy to represent and process using Euclidean geometry. Nevertheless, non-Euclidean spaces have recently been shown to provide significantly improved representations compared

¹Department of Electrical and Computer Engineering, University of Illinois at Urbana-Champaign, Urbana, IL, USA. Correspondence to: Puoya Tabaghi <tabaghi2@illinois.edu>.

Submitted to *Proceedings of the 38th International Conference on Machine Learning*, PMLR 139, 2021. Copyright 2021 by the author(s).

to Euclidean spaces for various data structures (Bronstein et al., 2017) and measurement modalities (e.g., metric and non-metric) (Tabaghi & Dokmanić, 2020b;a). Examples include *hyperbolic spaces*, suitable for representing human-interpretable images (Khrulkov et al., 2020) as well as hierarchical data associated with graphs (Nickel & Kiela, 2017; Sala et al., 2018); and *spherical spaces*, which are well-suited for capturing similarities in text embeddings and cycle-structures in graphs (Meng et al., 2019; Gu et al., 2018). Another important contribution in the area of non-Euclidean representation learning was described in (Gu et al., 2018), pertaining to learning methods for finding “good” mixed or hyperbolic representations for various types of complex heterogeneous datasets. All three spaces considered — hyperbolic, Euclidean, and spherical — have *constant curvatures* but differ in terms of their curvature signs (negative, zero and positive, respectively).

Despite these recent advances in nontraditional space data embeddings, almost all accompanying learning approaches for nonstandard space forms have focused on (heuristic) designs of neural network models for constant curvature spaces (Ganea et al., 2018; Chami et al., 2019; Tifrea et al., 2018; Liu et al., 2019; Shimizu et al., 2020; Meng et al., 2019). The most fundamental building blocks of these neural networks, the perceptron, has received surprisingly little attention outside the domain of learning in Euclidean spaces. Exceptions include two studies of linear classifiers (perceptrons and SVMs) in purely hyperbolic spaces (Cho et al., 2019; Weber et al., 2020). Although discussed within a limited context in (Skopek et al., 2020; Bachmann et al., 2020), classification in mixed product spaces remains largely unexplored, especially from the theoretical point of view. This is due to the highly nontrivial problem of defining inner products and distance functions on manifolds that allows for combining them in a unified manner within product spaces.

Here, we address for the first time the problem of designing linear classifiers for geodesically complete Riemannian manifolds with provable performance guarantees. Such spaces are endowed with logarithmic and exponential maps of crucial importance for establishing rigorous performance results. We first show that our classifiers for d -dimensional spaces can shatter $d+1$ points regardless of the curvature. We then describe the key ideas behind our analysis: Defining separation surfaces in constant curvature spaces directly

through the use of geodesics on Riemannian manifolds (this definition matches the one proposed in (Ganea et al., 2018; Shimizu et al., 2020) for implementing hyperbolic neural networks); and, introducing metrics that render distances in different spaces compatible with each other and integrate them into one “majority” signed distance. One particular distance-based classifier, our mixed-curvature perceptron, is extremely simple to implement, flexible and it relies on a small (reduced) number of parameters. The new perceptron algorithm comes with provable performance guarantees established via the use of specialized kernels and their Taylor series analysis. This proof technique significantly departs from methods proposed for classification in purely hyperbolic spaces (Cho et al., 2019; Weber et al., 2020) and it may be used as the first step towards a foundational study of other classification approaches, such as Support Vector Machines (SVMs) and neural networks.

From the practical point of view, we also demonstrate that our product space perceptron offers excellent performance on both synthetic product-space data and real-world datasets, such as MNIST (LeCun et al., 1998) and Omniglot (Lake et al., 2015) compared to similar methods in Euclidean spaces which ignore the geometry of the data.

The paper is organized as follows. In Sections 2 and 3 we review a special representation of linear classifiers in d -dimensional constant curvature spaces, e.g., Euclidean, hyperbolic and spherical spaces, and prove that distance-based classifiers have the same expressive power: Their Vapnik-Chervonenkis dimension equals $d + 1$. Section 4 contains our main results, a description of an approach for generalizing linear classifiers in space forms to product spaces and the first example of a mixed-curvature perceptron algorithm that performs provably optimal classification in a finite number of steps. Section 5 contains our simulation results pertaining to synthetic data, MNIST and Omniglot. All proofs are delegated to the Supplement.

2. Linear Classifiers in Euclidean Space

We start by revisiting the problem of linear classification in Euclidean spaces, i.e., in flat space forms. Finite-dimensional Euclidean spaces are inner product vector spaces over the reals. In contrast, hyperbolic and (hyper)spherical spaces do not have the structure of a vector space. Therefore, we first have to clarify what linear classification means in spaces with nonzero curvatures. To introduce our approach, we begin by recasting the definition of Euclidean linear classifiers in terms of commonly used concepts in differential geometry such as geodesics and Riemannian metrics (Ratcliffe et al., 1994). This will allow us to (1) present a unified way of viewing the classification procedure in metric spaces that are not necessarily vector spaces; (2) formalize *distance-based* linear classi-

fiers in space forms, i.e., classifiers that label data points based on their *signed distances* to the separation surface (Section 3); and (3) use the aforementioned classifiers as canonical building blocks of linear classifiers in product space forms (Section 4).

In a linear (more precisely, affine) binary classification problem we are given a set of N points in a Euclidean space and their binary labels, i.e., $(x_n, y_n) \in \mathbb{R}^d \times \{-1, 1\}$ and for $n \in [N] \stackrel{\text{def}}{=} \{1, \dots, N\}$. The goal is to learn a linear classifier that produces the most accurate estimate of the labels. We define a linear classifier with weight $w \in \mathbb{R}^d$ and bias $b \in \mathbb{R}$ as

$$l_{b,w}^{\mathbb{E}}(x) = \text{sgn}(w^\top x + b), \quad (1)$$

where $\|w\|_2 = 1$, and $l_{b,w}^{\mathbb{E}}(x)$ denotes the estimated label of $x \in \mathbb{R}^d$ under the given classifier parameters. The expression (1) may be reformulated in terms of a “point-line” pair as follows.

Let p be any point on the decision boundary and w a corresponding normal vector. Then, we have

$$l_{b,w}^{\mathbb{E}}(x) = \text{sgn}(\langle w, x - p \rangle), \quad (2)$$

where $b = -p^\top w$ and $\langle \cdot, \cdot \rangle$ stands for the standard inner product. Simply put, the linear classifier returns the sign of the inner product of tangent vectors of two straight lines,

$$\gamma_{p,x}(t) = (1 - t)p + tx \quad \text{and} \quad \gamma_n(t) = p + tw, \quad (3)$$

at their point of intersection $p \in \mathbb{R}^d$ (see Figure 1). Here, γ_n is the normal line and $\gamma_{p,x}$ is the line determined by p and the point x whose label we want to determine. Note that these lines are smooth curves parameterized by $t \in [0, 1]$ (or an open interval in \mathbb{R}), which we interpret as *time*. The linear classifier in (2) can be further reformulated as

$$l_{b,w}^{\mathbb{E}}(x) = \text{sgn}(\langle \frac{d}{dt} \gamma_{p,x}(t) |_{t=0}, \frac{d}{dt} \gamma_n(t) |_{t=0} \rangle),$$

where the derivative of a line $\gamma(t)$ at time 0 represents the *tangent vector* (or velocity) at the point $p = \gamma(0)$. This particular formulation leads to the following intuitive definition of linear classifiers in Euclidean spaces, which can

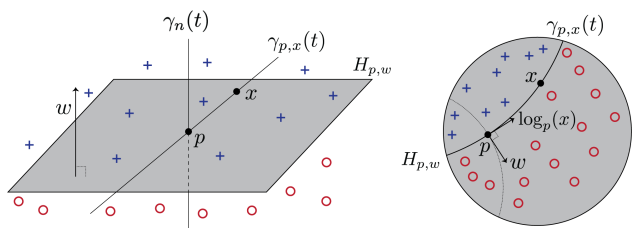


Figure 1. Linear classifiers in a 2-dimensional Euclidean space (left) and on a compact Riemannian manifold (right).

be generalized to other space forms, e.g., hyperbolic and spherical spaces.

Definition 1. A linear classifier in Euclidean space returns the sign of the inner product between tangent vectors of two straight lines described in (3) that meet at a unique point.

Often, we are interested in large-margin Euclidean linear classifiers for which we have $y_n \langle w, x_n - p \rangle \geq \varepsilon$, for all $n \in [N]$, and some margin $\varepsilon > 0$. For distance-based classifiers, we want ε to relate to the distance between the points x_n and the separation surface. For the classifier in (2), the distance between a point $x \in \mathbb{R}^d$ and the classification boundary, defined as $H_{p,w} = \{x \in \mathbb{R}^d : \langle w, x - p \rangle = 0\}$, can be computed as

$$\min_{y \in H_{p,w}} d(x, y) = |\langle w, x - p \rangle| = |w^\top x + b|.$$

Note that in the point-line definition (2), the point p can be anywhere on the decision boundary and it has d degrees of freedom whereas b from definition (1) is a scalar parameter. Therefore, we prefer definition (1) as it represents a distance-based Euclidean classifier with only $d + 1$ free parameters — w and b — and a norm constraint, i.e., $\|w\|_2 = 1$. In Section 3, we generalize this result by showing how to define distance-based classifiers in other d -dimensional space forms with $d + 1$ free parameters and a norm constraint.

3. Linear Classifiers in Space Forms

A space form is a complete, simply connected Riemannian manifold of dimension $d \geq 2$ and constant curvature. Space forms are equivalent to spherical, Euclidean, or hyperbolic spaces up to isomorphism (Lee, 2006). To define linear classifiers in space forms, we first review fundamental concepts from differential geometry such as geodesics, tangent vectors and Riemannian metrics needed to generalize the key terms in Definition 1. For a detailed review, see (Gallier & Quaintance, 2020; Ratcliffe et al., 1994).

Let \mathcal{M} be a Riemannian manifold and let $p \in \mathcal{M}$. The tangent space at the point p , denoted by $T_p \mathcal{M}$, is the collection of all tangent vectors at p . The Riemannian metric $g_p : T_p \mathcal{M} \times T_p \mathcal{M} \rightarrow \mathbb{R}$ is given by a positive-definite inner product in the tangent space $T_p \mathcal{M}$ which depends smoothly on the base point p . A Riemannian metric generalizes the notion of inner products for Riemannian manifolds. The norm of a tangent vector $v \in T_p \mathcal{M}$ is given by $\|v\| = \sqrt{g_p(v, v)}$. The length of a smooth curve $\gamma : [0, 1] \rightarrow \mathcal{M}$ (or path) can be computed as $L[\gamma] = \int_0^1 \|\gamma'(t)\| dt$. A geodesic γ_{p_1, p_2} on a manifold is the shortest length smooth path between the points $p_1, p_2 \in \mathcal{M}$,

$$\gamma_{p_1, p_2} = \arg \min_{\gamma} L[\gamma] : \gamma(0) = p_1, \gamma(1) = p_2;$$

this generalizes the notion of a straight line in Euclidean space. Next, consider a geodesic $\gamma(t)$ starting at p and with

initial velocity $v \in T_p \mathcal{M}$, e.g., $\gamma(0) = p$ and $\gamma'(0) = v$. The exponential map gives the position of this geodesic at $t = 1$, i.e., $\exp_p(v) = \gamma(1)$. Conversely, the logarithmic map is its inverse, i.e., $\log_p = \exp_p^{-1} : \mathcal{M} \rightarrow T_p \mathcal{M}$. In other words, for two points p and $x \in \mathcal{M}$, the logarithmic map $\log_p(x)$ gives the initial velocity (tangent vector) at which we can move — along the geodesic — from p to x in one time step.

In geodesically complete Riemannian manifolds, the exponential and logarithm maps are well-defined operators. Therefore, analogous to Definition 1, we can define a general notion of linear classifiers as described below.

Definition 2. Let (\mathcal{M}, g) be a geodesically complete Riemannian manifold, let $p \in \mathcal{M}$ and let $w \in T_p \mathcal{M}$ be a normal vector. A linear classifier $l_{p,w}$ over the manifold \mathcal{M} is defined as

$$l_{p,w}^{\mathcal{M}}(x) = \text{sgn}(g_p(w, \log_p(x))), \text{ where } x \in \mathcal{M}.$$

Despite its generality, Definition 2 has the following issues: (1) It does not formalize a distance-based classifier over \mathcal{M} since $|g_p(w, \log_p(x))|$ is not necessarily related to the distance of x to the decision boundary; (2) For a fixed $x \in \mathcal{M}$, the decision rule $g_p(w, \log_p(x))$ varies with the choice of p , an arbitrary point on the decision boundary; (3) Usually, we can represent a given decision boundary, e.g., $H_{p,w} = \{x \in \mathcal{M} : g_p(w, \log_p(x)) = 0\}$, with other parameters that have a smaller number of degrees of freedom compared to that of w and p required by Definition 2 (see the Euclidean linear classifiers defined in (2) and (1)).

We resolve these issues for linear classifiers in space forms in what follows. To this end, we use the notions and terminology described in Table 1. We also find the definition of null tangent subspaces at a point $p \in \mathcal{M}$ useful in our subsequent derivations.

Definition 3. Let (\mathcal{M}, g) be a manifold with Riemannian metric g . The null tangent subspace of $V \subseteq T_p \mathcal{M}$ equals

$$V^\perp = \{u \in T_p \mathcal{M} : g_p(u, v) = 0, \forall v \in V\}.$$

3.1. Spherical Spaces

Let $p \in \mathbb{S}^d$ and $w \in T_p \mathbb{S}^d = p^\perp$. The decision boundary is given by

$$\begin{aligned} H_{p,w} &= \left\{ x \in \mathbb{S}^d : \langle w, \frac{\theta}{\sin(\theta)}(x - p \cos \theta) \rangle = 0 \right\} \\ &\stackrel{(a)}{=} \{x \in \mathbb{S}^d : w^\top x = 0\} = \mathbb{S}^d \cap w^\perp, \end{aligned} \quad (4)$$

where (a) is due to the fact that $w \in p^\perp$. This formulation uses two parameters $p \in \mathbb{S}^d$ and $w \in T_p \mathbb{S}^d$ to define the decision boundary (4). But, we can characterize the same

Table 1. Key concepts used to define linear classifiers in Euclidean (\mathbb{R}^d), spherical (\mathbb{S}^d), and hyperbolic ('Loid model, \mathbb{L}^d) spaces.

\mathcal{M}	$T_p\mathcal{M}$	$g_p(u, v)$	$\log_p(x) : \theta = d(x, p)$	$\exp_p(v)$	$d(x, p)$	$\gamma_{p,x}(t)$
\mathbb{R}^d	\mathbb{R}^d	$\langle u, v \rangle$	$x - p$	$p + v$	$\ x - p\ _2$	$(1 - t)p + tx$
\mathbb{S}^d	p^\perp	$\langle u, v \rangle$	$\frac{\theta}{\sin(\theta)}(x - p \cos \theta)$	$\cos \ v\ p + \sin(\ v\) \frac{v}{\ v\ }$	$\text{acos}(\langle x, p \rangle)$	$\frac{\sin(\theta(1-t))}{\sin \theta} p + \frac{\sin(\theta t)}{\sin \theta} x$
\mathbb{L}^d	p^\perp	$[u, v]$	$\frac{\theta}{\sinh(\theta)}(x - p \cosh \theta)$	$\cosh \ v\ p + \sinh(\ v\) \frac{v}{\ v\ }$	$\text{acosh}(-[x, p])$	$\frac{\sinh(\theta(1-t))}{\sinh \theta} p + \frac{\sinh(\theta t)}{\sinh \theta} x$

boundary with fewer parameters. Note that for any $w \in \mathbb{R}^{d+1}$, we can pick an arbitrary base vector $p \in w^\perp \cap \mathbb{S}^d$, and this ensures that $w \in T_p\mathbb{S}^d$. Therefore, without loss of generality, we can define the decision boundary using only one vector $w \in \mathbb{R}^{d+1}$, which has $d + 1$ degrees of freedom. In Proposition 1, we identify a specific choice of $p \in w^\perp \cap \mathbb{S}^d$ that allows us to classify each data point based on its signed distance from the classification boundary.

Proposition 1. *Let $p \in \mathbb{S}^d$, $w \in T_p\mathbb{S}^d = p^\perp$, and let $H_{p,w}$ be the decision boundary as previously defined. If $\|w\|_2 = 1$, then*

$$\min_{y \in H_{p,w}} d(x, y) = \text{asin}|w^\top x| = |g_{p_\circ}^{\mathbb{S}}(w, \log_{p_\circ}(x))|,$$

where $g^{\mathbb{S}}$ is the Riemannian metric for a spherical space given in Table 1, and $p_\circ = \|P_w^\perp x\|^{-1} P_w^\perp x \in w^\perp \cap \mathbb{S}^d$. Note that the projection operator is defined as $P_w^\perp x = x - \langle x, w \rangle w$.

It is important to point out that the classification boundary is invariant with respect to the choice of the base vectors, i.e., $H_{p,w} = H_{p_\circ,w}$. From Proposition 1, if we have

$$y_n \text{asin}(w^\top x_n) \geq \varepsilon, \quad \forall n \in [N],$$

then all data points $\{x_n\}_{n \in [N]}$ are correctly classified and have the minimum distance of ε to the classification boundary. As a result, we have the following definition.

Definition 4. *Let $w \in \mathbb{R}^{d+1}$ with $\|w\|_2 = 1$. A spherical linear classifier is defined as*

$$l_w^{\mathbb{S}}(x) = \text{sgn}(\text{asin}(w^\top x)).$$

3.2. Hyperbolic Spaces

The 'Loid model of d -dimensional hyperbolic space (Cannon et al., 1997) is a Riemannian manifold $\mathcal{L}^d = (\mathbb{L}^d, g^{\mathbb{H}})$ for which $\mathbb{L}^d = \{x \in \mathbb{R}^{d+1} : [x, x] = -1, x_1 > 0\}$, and $g_p^{\mathbb{H}}(u, v)$ corresponds to the Lorentzian inner product of u and $v \in T_p\mathbb{L}^d = p^\perp$, defined as

$$[u, v] = u^\top H v, \quad H = \begin{pmatrix} -1 & 0^\top \\ 0 & I_d \end{pmatrix}, \quad (5)$$

where I_d is a $d \times d$ identity matrix. Let $p \in \mathbb{L}^d$ and $w \in T_p\mathbb{L}^d$. The classification boundary of interest is given by

$$\begin{aligned} H_{p,w} &= \left\{ x \in \mathbb{L}^d : [w, \frac{\theta}{\sinh(\theta)}(x - p \cosh \theta)] = 0 \right\} \\ &= \{x \in \mathbb{L}^d : [w, x] = 0\} = \mathbb{L}^d \cap w^\perp. \end{aligned}$$

Similar to the spherical case, we can simplify the formulation as follows. If w is a time-like vector — a vector that satisfies $w \in \{x : [x, x] > 0\}$ (Ratcliffe et al., 1994) — and $p \in \mathbb{L}^d \cap w^\perp$, then we have $w \in T_p\mathbb{L}^d$. In Proposition 2, we compute a specific $p_\circ \in \mathbb{L}^d \cap w^\perp$ to arrive at a distance-based hyperbolic classifier.

Proposition 2. *Let $p \in \mathbb{L}^d$, $w \in T_p\mathbb{L}^d = p^\perp$, and let $H_{p,w}$ be an affine subspace as defined before. If $[w, w] = 1$, then,*

$$\min_{y \in H_{p,w}} d(x, y) = \text{asinh}|[w, x]| = |g_{p_\circ}^{\mathbb{H}}(w, \log_{p_\circ}(x))|$$

where $g^{\mathbb{H}}$ is the Riemannian metric for the hyperbolic space given in Table 1, and $p_\circ = \|P_w^\perp x\|^{-1} P_w^\perp x \in w^\perp \cap \mathbb{L}^d$. Note that $P_w^\perp x$ is the orthogonal projection of x onto w^\perp , i.e., $P_w^\perp x = x - [x, w]w$. Therefore, $p_\circ = \sqrt{\frac{1}{1+[x,w]^2}}(x - [x, w]w)$.

As a result, we have the following formal definition of a distance-based linear classifier in a hyperbolic space.

Definition 5. *Let $w \in \mathbb{R}^{d+1}$ with $[w, w] = 1$. A linear classifier in hyperbolic space is defined as*

$$l_w^{\mathbb{H}}(x) = \text{sgn}(\text{asinh}([w, x])).$$

Figure 2 illustrates linear classifiers in 2-dimensional hyperbolic, Euclidean, and spherical spaces.

From the previous discussion, we can easily deduce the fact that *linear classifiers in d -dimensional space forms can be characterized with $d + 1$ free parameters and a norm constraint*. This supports the result established below pertaining to the Vapnik-Chervonenkis dimension (Vapnik, 2013) of linear classifiers in space forms.

Theorem 1. *The VC dimension of a linear classifier in a d -dimensional space form is $d + 1$.*

Next, we show how these classifiers, that have the same expressive power, can be “mixed” to define a linear classifier in product space forms.

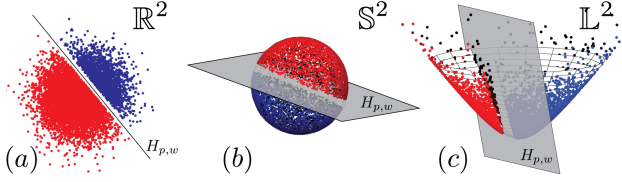


Figure 2. Linear classifiers in 2-dimensional (a) Euclidean, (b) spherical, and (c) hyperbolic spaces.

4. Linear Classifiers in Product Space Forms

Definition 2 of linear classifiers applies to all geodesically complete Riemannian manifolds but our focus will be on linear classifiers in product space forms. We describe the first perceptron algorithm for such spaces that *provably* learns an optimal classifier for linearly separable points in a finite number of iterations.

Consider a collection of Euclidean, spherical, and hyperbolic manifolds, e.g., $(\mathbb{E}^{d_{\mathbb{E}}}, g^{\mathbb{E}})$, $(\mathbb{S}^{d_{\mathbb{S}}}, g^{\mathbb{S}})$, $(\mathbb{H}^{d_{\mathbb{H}}}, g^{\mathbb{H}})$ with sectional curvatures 0, 1, -1 , respectively (later in this section, we provide a simple explanation how to generalize our results for space forms with arbitrary curvatures). The Euclidean manifold is simply $\mathbb{R}^{d_{\mathbb{E}}}$ while the hyperbolic space is the 'Loid model $\mathbb{L}^{d_{\mathbb{H}}}$ (see Table 1).

The product manifold $\mathcal{M} = \mathbb{E}^{d_{\mathbb{E}}} \times \mathbb{S}^{d_{\mathbb{S}}} \times \mathbb{H}^{d_{\mathbb{H}}}$ admits a canonical Riemannian metric g , called the *product Riemannian metric*. The tangent space of \mathcal{M} at a point $p = (p_{\mathbb{E}}, p_{\mathbb{S}}, p_{\mathbb{H}})$ can be decomposed as

$$T_p \mathcal{M} = \bigoplus_{S \in \{\mathbb{E}, \mathbb{S}, \mathbb{H}\}} T_{p_S} S^{d_S} \quad (\text{Tu, 2011}), \quad (6)$$

where the right-hand side expression is the direct sum \bigoplus of individual tangent spaces $T_{p_{\mathbb{E}}} \mathbb{E}^{d_{\mathbb{E}}}$, $T_{p_{\mathbb{S}}} \mathbb{S}^{d_{\mathbb{S}}}$, and $T_{p_{\mathbb{H}}} \mathbb{H}^{d_{\mathbb{H}}}$. Let $u, v \in T_p \mathcal{M}$. The Riemannian metric used on \mathcal{M} is

$$g_p(u, v) = \sum_{S \in \{\mathbb{E}, \mathbb{S}, \mathbb{H}\}} g_{p_S}^S(u_S, v_S), \quad (7)$$

where $u = (u_{\mathbb{E}}, u_{\mathbb{S}}, u_{\mathbb{H}})$, $v = (v_{\mathbb{E}}, v_{\mathbb{S}}, v_{\mathbb{H}})$, and $p = (p_{\mathbb{E}}, p_{\mathbb{S}}, p_{\mathbb{H}})$.

Based on the discussion from the previous section, in order to describe linear classifiers on the above manifold \mathcal{M} , we first need to identify an appropriate logarithmic map (see Definition 2). For this purpose, we invoke the following known result that formalizes geodesics, exponential and logarithmic maps on \mathcal{M} .

Fact 1. (Gallier & Quaintance, 2020) Let $\mathcal{M} = \mathbb{E}^{d_{\mathbb{E}}} \times \mathbb{S}^{d_{\mathbb{S}}} \times \mathbb{H}^{d_{\mathbb{H}}}$ be a product manifold with Riemannian metric given by (7). Then, the geodesics, exponential, and logarithmic maps on \mathcal{M} are simply the concatenation of the corresponding maps of the individual space forms in \mathcal{M} ,

i.e.,

$$\begin{aligned} \gamma(t) &= (\gamma_{\mathbb{E}}(t), \gamma_{\mathbb{S}}(t), \gamma_{\mathbb{H}}(t)) \\ \exp_p(v) &= (\exp_{p_{\mathbb{E}}}(v_{\mathbb{E}}), \exp_{p_{\mathbb{S}}}(v_{\mathbb{S}}), \exp_{p_{\mathbb{H}}}(v_{\mathbb{H}})) \\ \log_p(x) &= (\log_{p_{\mathbb{E}}}(x_{\mathbb{E}}), \log_{p_{\mathbb{S}}}(x_{\mathbb{S}}), \log_{p_{\mathbb{H}}}(x_{\mathbb{H}})) \end{aligned}$$

where $p = (p_{\mathbb{E}}, p_{\mathbb{S}}, p_{\mathbb{H}})$, $x = (x_{\mathbb{E}}, x_{\mathbb{S}}, x_{\mathbb{H}}) \in \mathcal{M}$, $v = (v_{\mathbb{E}}, v_{\mathbb{S}}, v_{\mathbb{H}}) \in T_p \mathcal{M}$, and $\gamma_{\mathbb{E}}, \gamma_{\mathbb{S}}, \gamma_{\mathbb{H}}$ are geodesics in Euclidean, spherical, and hyperbolic spaces. Moreover, a distance function on the product manifold may be defined according to $d(x, y)^2 = \sum_{S \in \{\mathbb{E}, \mathbb{S}, \mathbb{H}\}} d_S(x_S, y_S)^2$, for $x, y \in \mathcal{M}$, where d_S is the distance function of S as in Table 1.

Combining the results regarding distance-based linear classifiers in space forms (Section 3), the definition of tangent product spaces in terms of the product of tangent spaces in (6), and the choice of the Riemannian metrics given in Table 1, we arrive at the following formulation for a product space linear classifier.

Definition 6. Let $\mathcal{M} = \mathbb{E}^{d_{\mathbb{E}}} \times \mathbb{S}^{d_{\mathbb{S}}} \times \mathbb{H}^{d_{\mathbb{H}}}$ be the product manifold with the Riemannian metric given by (7). The product linear classifier on \mathcal{M} takes the form

$$l_w^{\mathcal{M}}(x) = \text{sgn}(w_{\mathbb{E}}^{\top} x_{\mathbb{E}} + b + \text{asinh}(w_{\mathbb{S}}^{\top} x_{\mathbb{S}}) + \text{asinh}([w_{\mathbb{H}}, x_{\mathbb{H}}]))$$

where $x = (x_{\mathbb{E}}, x_{\mathbb{S}}, x_{\mathbb{H}})$, $w = (w_{\mathbb{E}}, b, w_{\mathbb{S}}, w_{\mathbb{H}})$, and $w_{\mathbb{E}}, w_{\mathbb{S}}$ and $w_{\mathbb{H}}$ have unit norms.

This classifier can be associated with three linear classifiers for Euclidean, hyperbolic, and spherical spaces. For a point $x = (x_{\mathbb{E}}, x_{\mathbb{S}}, x_{\mathbb{H}}) \in \mathcal{M}$, the product space classifier takes a weighted vote based on the signed distances of each component (e.g., $x_{\mathbb{E}}$, $x_{\mathbb{S}}$, and $x_{\mathbb{H}}$) to its corresponding classifier's boundary (Figure 3 illustrates two classifiers in product space forms).

The choice of the Riemannian metric in Equation (7) — and hence the classification criteria — comes with “compatibility” issues that arise from possibly vastly different ranges/variances of each component, e.g., $x_{\mathbb{E}}$, $x_{\mathbb{S}}$, and $x_{\mathbb{H}}$. For instance, we know that the spherical space is compact and that the distance of an arbitrary point to any classification boundary is bounded. More precisely, for a sphere with

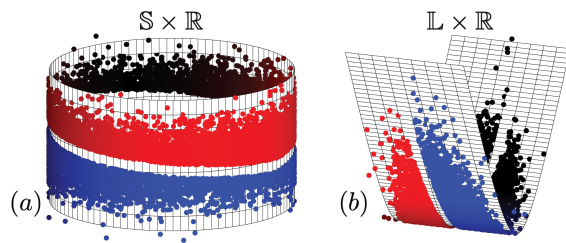


Figure 3. Examples of linear classifiers in product space forms. (a): $\mathbb{S} \times \mathbb{R}$ and (b): $\mathbb{L} \times \mathbb{R}$. A hyperbolic space has dimension ≥ 2 and in (b) we reduced it for visualization purposes only.

unit radius, $\min_{y \in H_{p,w}} d(x, y) \leq \pi$. In comparison, hyperbolic and Euclidean spaces are not compact and distances can be potentially unbounded. Hence, directly using Definition 6 may lead to a classification process that can be dominated by the component with the largest variance.

One can resolve the issue of distance ‘‘incompatibility’’ by uniformly scaling the Riemannian metrics of each space form. For example, consider the Euclidean space \mathbb{R}^d with Riemannian metric defined as

$$g_{p_{\mathbb{E}}}^{\mathbb{E}}(u, v) = \alpha_{\mathbb{E}} u^{\top} v,$$

where $p_{\mathbb{E}} \in \mathbb{R}^d$, $u, v = T_{p_{\mathbb{E}}} \mathbb{R}^d = \mathbb{R}^d$, and $\alpha_{\mathbb{E}} > 0$. This metric allows for scaling the distances between two points, or the length of the geodesic between them according to

$$d(x, y) = \alpha_{\mathbb{E}} \|x - y\|_2, \quad \text{for } x, y \in \mathbb{R}^d.$$

This straightforward observation is useful because it does not change the form of the geodesics, tangent spaces, exponential and logarithmic maps (see Section 3). Therefore, for a product space form $\mathcal{M} = \mathbb{E}^{d_{\mathbb{E}}} \times \mathbb{S}_{C_{\mathbb{S}}}^{d_{\mathbb{S}}} \times \mathbb{H}_{C_{\mathbb{H}}}^{d_{\mathbb{H}}}$ we choose the Riemannian metric defined as

$$g_p(u, v) = \sum_{S \in \{\mathbb{E}, \mathbb{S}, \mathbb{H}\}} \alpha_S g_{p_S}^S(u_S, v_S), \quad (8)$$

where $u = (u_{\mathbb{E}}, u_{\mathbb{S}}, u_{\mathbb{H}})$, $v = (v_{\mathbb{E}}, v_{\mathbb{S}}, v_{\mathbb{H}})$, $p = (p_{\mathbb{E}}, p_{\mathbb{S}}, p_{\mathbb{H}})$, and $\alpha_{\mathbb{E}}$, $\alpha_{\mathbb{S}}$, and $\alpha_{\mathbb{H}}$ are positive weights. Accordingly, a linear classifier on \mathcal{M} may be written as

$$l_w^{\mathcal{M}}(x) = \operatorname{sgn}(w_{\mathbb{E}}^{\top} x_{\mathbb{E}} + b + \alpha_{\mathbb{S}} \operatorname{asin}(w_{\mathbb{S}}^{\top} x_{\mathbb{S}}) + \alpha_{\mathbb{H}} \operatorname{asinh}([w_{\mathbb{H}}, x_{\mathbb{H}}])),$$

where $\|w_{\mathbb{E}}\|_2 = \alpha_{\mathbb{E}}$, and $w_{\mathbb{S}}$ and $w_{\mathbb{H}}$ have unit norms.

In the final step, we generalize the proposed linear classifier to account for space forms with arbitrary sectional curvatures. For detailed derivations, the interested reader is referred to the Supplement.

Proposition 3. *Let $\mathbb{S}_{C_{\mathbb{S}}}^{d_{\mathbb{S}}}$ and $\mathbb{H}_{C_{\mathbb{H}}}^{d_{\mathbb{H}}}$ be spherical and hyperbolic spaces with curvatures $C_{\mathbb{S}} > 0$, and $C_{\mathbb{H}} < 0$. Let $\mathcal{M} = \mathbb{E}^{d_{\mathbb{E}}} \times \mathbb{S}_{C_{\mathbb{S}}}^{d_{\mathbb{S}}} \times \mathbb{H}_{C_{\mathbb{H}}}^{d_{\mathbb{H}}}$ be the product manifold with Riemannian metric given by (7). A linear classifier on \mathcal{M} under the given metric is defined as*

$$l_w^{\mathcal{M}}(x) = \operatorname{sgn}(w_{\mathbb{E}}^{\top} x_{\mathbb{E}} + b + \sqrt{C_{\mathbb{S}}} \operatorname{asin}(w_{\mathbb{S}}^{\top} x_{\mathbb{S}}) + \sqrt{-C_{\mathbb{H}}} \operatorname{asinh}([w_{\mathbb{H}}, x_{\mathbb{H}}])),$$

where $x = (x_{\mathbb{E}}, x_{\mathbb{S}}, x_{\mathbb{H}})$, $w = (w_{\mathbb{E}}, b, w_{\mathbb{S}}, w_{\mathbb{H}})$, and $w_{\mathbb{E}}$, $w_{\mathbb{S}}$ and $w_{\mathbb{H}}$ have norms of 1, $\sqrt{C_{\mathbb{S}}}$, and $\sqrt{-C_{\mathbb{H}}}$, respectively.

4.1. The Mixed-Curvature Perceptron

We now turn our attention to an algorithmic solution to the general linear classification problem in a product space form

$\mathcal{M} = \mathbb{E}^{d_{\mathbb{E}}} \times \mathbb{S}_{C_{\mathbb{S}}}^{d_{\mathbb{S}}} \times \mathbb{H}_{C_{\mathbb{H}}}^{d_{\mathbb{H}}}$ and with Riemannian metric (8). To establish provable performance guarantees, we assume that the datasets of interest have an $\varepsilon > 0$ margin, i.e.,

$$y(w_{\mathbb{E}}^{\top} x_{\mathbb{E}} + b + \alpha_{\mathbb{S}} \sqrt{C_{\mathbb{S}}} \operatorname{asin}(w_{\mathbb{S}}^{\top} x_{\mathbb{S}}) + \alpha_{\mathbb{H}} \sqrt{-C_{\mathbb{H}}} \operatorname{asinh}([w_{\mathbb{H}}, x_{\mathbb{H}}])) \geq \varepsilon, \quad \forall (x, y) \in \mathcal{X}, \quad (9)$$

where \mathcal{X} is the set of labeled training data, $\|w_{\mathbb{E}}\|_2 = \alpha_{\mathbb{E}}$, $\|w_{\mathbb{S}}\|_2 = \sqrt{C_{\mathbb{S}}}$, and $\sqrt{[w_{\mathbb{H}}, x_{\mathbb{H}}]} = \sqrt{-C_{\mathbb{H}}}$. It is important to observe that the classification function is nonlinear in $w_{\mathbb{S}}$ and $w_{\mathbb{E}}$ and that we require equality constraints for all the weights involved.

To analyze the classifier and allow for sequential updates of its parameters, we propose to relax the norm constraints and use a kernel-based approach that mimics the Euclidean perceptron updates in Reproducing Kernel Hilbert Space (RKHS), e.g., \mathcal{H} . We seek a map $\phi : \mathcal{M} \rightarrow \mathcal{H}$, where \mathcal{H} is a RKHS. The goal is to represent the classifier in (9) as an inner product of two vectors in \mathcal{H} , i.e., $l_w^{\mathcal{M}}(x) = \langle \phi(w), \phi(x) \rangle_{\mathcal{H}}$, where $\langle \cdot, \cdot \rangle_{\mathcal{H}}$ is the inner product defined on \mathcal{H} . The kernels $K_{\mathbb{E}}(w_{\mathbb{E}}, x_{\mathbb{E}}) = w_{\mathbb{E}}^{\top} x_{\mathbb{E}} + b$ and $K_{\mathbb{S}}(w_{\mathbb{S}}, x_{\mathbb{S}}) = \operatorname{asin}(w_{\mathbb{S}}^{\top} x_{\mathbb{S}})$ are symmetric and positive definite. Hence, they lend themselves to the construction of a valid RKHS. Unfortunately, $K_{\mathbb{H}}(w_{\mathbb{H}}, x_{\mathbb{H}}) = \operatorname{asinh}(w_{\mathbb{H}}^{\top} x_{\mathbb{H}})$ is an indefinite kernel. Our solution to this problem is to introduce an indefinite operator $M : \mathcal{H}' \rightarrow \mathcal{H}'$, where $\mathcal{H}' \supseteq \mathcal{H}$ is the set of functions $\mathcal{M} \rightarrow \mathbb{R}$, and $M^{\top} M = \operatorname{Id}$ with Id denoting the identity operator. The operator M can be obtained by analyzing the Taylor series of $\operatorname{asinh}(\cdot)$. Then, the classifier (9) may be written as

$$l_w^{\mathcal{M}}(x) = \operatorname{sgn}(\langle \phi(w), M\phi(x) \rangle_{\mathcal{H}}), \quad (10)$$

where $\phi(w), \phi(x) \in \mathcal{H}'$ so that the inner product $\langle \cdot, M \cdot \rangle_{\mathcal{H}}$ is well-defined on \mathcal{H}' . Accordingly, we use the following update rule in \mathcal{H}'

$$w_{\phi}^{k+1} = w_{\phi}^k + y_n M\phi(x_n) \quad (11)$$

for any misclassified point, i.e., any point that satisfies $y_n \langle w_{\phi}^k, M\phi(x_n) \rangle_{\mathcal{H}} < 0$. Note that the operator M in the update rule (11) ensures that the *definite inner product* between w_{ϕ}^k and the *true* parameter $\phi(w)$ increases linearly with k . As a result, in Theorem 2, we show that the proposed update rule ensures that the product space perceptron in Algorithm 1 converges in finite number of steps.

Theorem 2. *Let $\{x_n, y_n\}_{n=1}^N$ be points in a compact subset of \mathcal{M} , with labels in $\{-1, 1\}$. If the point set is ε -margin linearly separable and $\|w_{\mathbb{H}}\|_2 \leq \max_{n \in [N]} \|x_{n,\mathbb{H}}\|_2$, then Algorithm 1 converges in $O(\frac{1}{\varepsilon^2})$ steps.*

For a more technical discussion of the operator M and the proof the interested reader is referred to the Supplement. As a final note, observe that the update rule in (11) is executed

Algorithm 1 Mixed-Curvature Perceptron

Input: $\{x_n, y_n\}_{n=1}^N$: a set of pairs of point-labels in $\mathcal{M} \times \{-1, 1\}$;

Initialization: $k = 0, n = 1, R_{\mathbb{H}} = \max_{n \in [N]} \|x_{n, \mathbb{H}}\|$;

repeat

if $\text{sgn}(l_k(x_n)) \neq y_n$ **then**

$\delta(x) \stackrel{\text{def}}{=} y_n (x_{n, \mathbb{E}}^\top x_{\mathbb{E}} + 1 + \alpha_{\mathbb{S}} \sqrt{C_{\mathbb{S}}} \sin(C_{\mathbb{S}} x_{n, \mathbb{S}}^\top x_{\mathbb{S}}) + \alpha_{\mathbb{H}} \sqrt{-C_{\mathbb{H}}} \sin(\frac{\langle x_{n, \mathbb{H}}, x_{\mathbb{H}} \rangle}{R_{\mathbb{H}}^2}))$: $x = (x_{\mathbb{E}}, x_{\mathbb{S}}, x_{\mathbb{H}})$;

$l_{k+1}(x) = l_k(x) + \delta(x)$;

$k = k + 1$;

end if

$n = \text{mod}(n, N) + 1$;

until Convergence criteria is met.

in \mathcal{H}' . However, the decision rule (10) only depends on the inner products of vectors in \mathcal{H}' . Therefore, one can implement the classification rule for a new data point $x \in \mathcal{M}$ via evaluation of the kernel function at x and the misclassified training data points, i.e., $K(x, x_n)$ (see Algorithm 1).

4.2. Discussion

Linear classifiers in spherical spaces have been studied in a number of works (Novikoff, 1963; Dasgupta et al., 2009), while more recent work has focused on linear classifiers in the Poincaré model of hyperbolic spaces, in the context of hyperbolic neural networks (Ganea et al., 2018). A purely hyperbolic perceptron (in the same 'Loid model used in this work) was described in (Weber et al., 2020). The proposed update rule reads as

$$u^k = w^k + y_n x_n \text{ if } -y_n [w^k, x_n] < 0 \quad (12)$$

$$w^{k+1} = u^k / \min\{1, \sqrt{[u^k, u^k]}\}, \quad (13)$$

where (13) is a “normalization step”. Unfortunately, the above update rule does not allow the hyperbolic perceptron algorithm (Equations (12) and (13)) to converge, which is due to the choice of the update direction. The convergence issue is also illustrated by the following two examples.

Let $x_1 = e_1 \in \mathbb{L}^2$, where e_1 is a standard basis vector with label $y_1 = 1$. We choose the initial vector in the update rule to be $w^0 = e_2$, as described in the proof (Weber et al., 2020). In the first iteration, we must hence update w^0 since $[w^0, x_1] = 0$. From (12), we have $u^0 = e_1 + e_2$, and $[u^0, u^0] = 0$. This means that $w^1 = \frac{1}{\sqrt{[u^0, u^0]}} u^0$ is clearly ill-defined. As another example, let w^* be the optimal vector with which we can classify all data points with margin ε . If we simply choose $w^0 = 0$, then we can satisfy the required condition $[w^0, w^*] \geq 0$ postulated for the hyperbolic perceptron. This leads to $u^0 = x_1$. Then, for any $x_1 \in \mathbb{L}^2$, we have $[x_1, x_1] = -1$, which leads to

Algorithm 2 Hyperbolic Perceptron

Input: $\{x_n, y_n\}_{n=1}^N$: a set of point-labels in $\mathbb{H}_{C_{\mathbb{H}}}^{d_{\mathbb{H}}} \times \{-1, 1\}$.

Initialization: $w^0 = 0 \in \mathbb{R}^{d_{\mathbb{H}}+1}, k = 0, n = 1$.

repeat

if $\text{sgn}([w^k, x_n]) \neq y_n$ **then**

$w^{k+1} = w^k + y_n H x_n$;

$k = k + 1$;

end if

$n = \text{mod}(n, N) + 1$;

until Convergence criteria is met.

a normalization factor $\sqrt{[u^0 u^0]}$ that is a complex number. Further simulation evidence that the algorithm does not converge is presented in the Supplement.

Given our mixed-curvature classifier derivations, we propose a modified update rule for a purely hyperbolic perceptron which is of independent interest and listed in Algorithm 2. Our hyperbolic perceptron uses a modified update direction and provably converges; see Theorem 3. The proof follows a similar approach as the one used for the Euclidean counterpart.

Theorem 3. Let $\{x_n, y_n\}_{n=1}^N$ be a set of N points from a bounded subset of $\mathbb{H}_{C_{\mathbb{H}}}^{d_{\mathbb{H}}}$, and their corresponding labels in $\{-1, 1\}$. If the point set is linearly separable by margin ε . The hyperbolic perceptron converges in $O\left(\frac{1}{\sinh^2(\varepsilon)}\right)$ steps.

5. Numerical Experiments

We illustrate the practical performance of our mixed-curvature perceptron Algorithm 1 on both synthetic and real-world datasets. In order to establish the benefits of mixed-curvature embeddings and learning, we compare our results with those obtained by using a Euclidean perceptron. As is a common approach for perceptron methods, we evaluate the classification accuracy on the training sets. To ensure a fair comparison, we restrict the latent dimension of the embeddings of both methods to be the same, meaning that data points lie in $\mathbb{E}^{d_{\mathbb{E}}} \times \mathbb{S}^{d_{\mathbb{S}}} \times \mathbb{H}^{d_{\mathbb{H}}}$ for the mixed-curvature perceptron and in $\mathbb{E}^{d_{\mathbb{E}}+d_{\mathbb{S}}+d_{\mathbb{H}}}$ for the Euclidean perceptron. We present a more detailed discussion and additional results in the Supplement.

5.1. Synthetic Datasets

We generate binary-labeled synthetic data satisfying a ε -margin assumption as follows. First, we randomly and independently sample N points from a Gaussian distribution in each of the three spaces $\mathbb{E}^2, \mathbb{E}^3, \mathbb{E}^3$; subsequently, we project the points in \mathbb{E}^2 and \mathbb{E}^3 onto \mathbb{S}_1^2 and \mathbb{H}_{-1}^2 , respectively. Then, we concatenate the coordinates from the three space form components to obtain the mixed-curvature

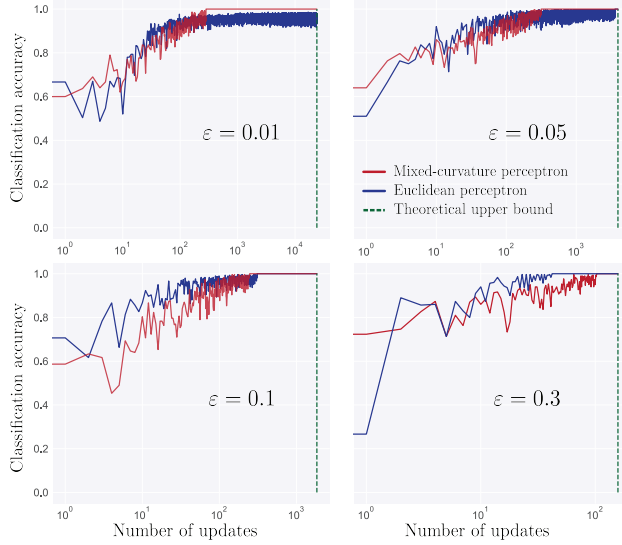


Figure 4. Classification accuracy after each update of the mixed-curvature and Euclidean perceptron algorithms for $N = 300$ and different values of ε .

embeddings. Finally, we randomly generate the optimal decision hyperplane $w^* = (w_{\mathbb{E}}^*, 0, w_{\mathbb{S}}^*, w_{\mathbb{H}}^*)$ under the constraints stated in Theorem 2 and assign binary labels to data points. To ensure that the ε -margin assumption is satisfied, we translate points that violate this assumption.

We use the same data for both the mixed-curvature and Euclidean perceptron to demonstrate the efficiency and performance gains of the former method. This is because our method respects the geometry of data, whereas the purely Euclidean setting assumes input data lies in \mathbb{E}^8 . In Figure 4, we show four different typical experimental convergence plots for $N = 300$ points with the same optimal decision hyperplane w^* , but with different separation margins, i.e., ε . We observe that the number of updates made by the mixed-curvature perceptron is always smaller than the theoretical upper bound provided in Theorem 2. When the margin is small, the data is not linearly separable in Euclidean space and the Euclidean perceptron does not converge to a 100% accurate solution. As ε increases, the data becomes easy to classify for both algorithms, and the number of updates made by the Euclidean perceptron decreases.

5.2. Real-World Datasets

In this section, we work with datasets containing more than two classes. To enable K -class perceptron classification, we use K binary classifiers — represented by parameters $w^{(i)}, i = 1, \dots, K$ — that are independently trained on the same training set to separate each single class from the remaining classes. For each classifier, we transform the resulting prediction scores into probabilities via the Platt scaling technique (Platt et al., 1999). The predicted labels

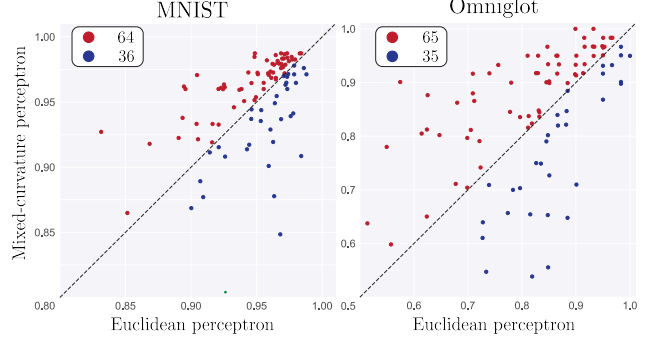


Figure 5. Comparison of Macro F1 scores of the mixed-curvature and Euclidean perceptron on MNIST and Omniglot.

are decided by maximum a posteriori criteria, using the probability of each class.

The datasets of interest include MNIST, containing images of handwritten digits (LeCun et al., 1998), and Omniglot, containing handwritten characters from a variety of world alphabets (Lake et al., 2015). As suggested in (Salakhutdinov & Murray, 2008) and (Burda et al., 2016), we downsample each image (in both datasets) to 28×28 pixels and preprocess it by a dynamic-binarization procedure. Then we use the mixed-curvature VAE from (Skopek et al., 2020) with default parameters to obtain a mixed-curvature embedding in $\mathbb{E}^2 \times \mathbb{S}^2 \times \mathbb{H}^2$ and Euclidean embedding in \mathbb{E}^6 . In these datasets, embedded points from different classes are not guaranteed to be linearly separable. Hence, we set both perceptron algorithms to terminate after going through a fixed maximum number of passes. Subsequently, we compute the Macro F1 scores to determine the quality of the learned linear classifiers. For simplicity, we only report ternary classification results for both datasets, including 500 points from three randomly chosen classes from MNIST and 20 points from three randomly chosen classes from Omniglot.

We show the performance of the ternary classifiers in Figure 5. This is obtained by randomly selecting 100 sets of three classes; each point in the figure corresponds to one such combination, and its coordinate value equals the averaged Macro F1 score of three independent runs. Red-colored points indicate better performance of the mixed-curvature perceptron, while blue-colored points indicate better performance of the Euclidean perceptron. We observe that the mixed-curvature perceptron classifies almost twice as many sets with higher accuracy compared to its Euclidean counterpart. Our experiments also reveal that although the differences in the log-likelihoods used to measure the quality of mixed-curvature and Euclidean VAE embeddings are small (as reported in (Skopek et al., 2020) and shown in the Supplement), the performance gain of our mixed-curvature perceptron compared to a Euclidean perceptron can be as high as 9.56% for MNIST and 32.63% for Omniglot.

References

Bachmann, G., Bécigneul, G., and Ganea, O. Constant curvature graph convolutional networks. In *International Conference on Machine Learning*, pp. 486–496. PMLR, 2020.

Bronstein, M. M., Bruna, J., LeCun, Y., Szlam, A., and Vandergheynst, P. Geometric deep learning: going beyond euclidean data. *IEEE Signal Processing Magazine*, 34(4):18–42, 2017.

Burda, Y., Grosse, R., and Salakhutdinov, R. Importance weighted autoencoders. In *International Conference on Learning Representations*, 2016.

Cannon, J. W., Floyd, W. J., Kenyon, R., Parry, W. R., et al. Hyperbolic geometry. *Flavors of geometry*, 31:59–115, 1997.

Chami, I., Ying, Z., Ré, C., and Leskovec, J. Hyperbolic graph convolutional neural networks. In *Advances in neural information processing systems*, pp. 4868–4879, 2019.

Cho, H., DeMeo, B., Peng, J., and Berger, B. Large-margin classification in hyperbolic space. In *The 22nd International Conference on Artificial Intelligence and Statistics*, pp. 1832–1840. PMLR, 2019.

Dasgupta, S., Kalai, A. T., and Tauman, A. Analysis of perceptron-based active learning. *Journal of Machine Learning Research*, 10(2), 2009.

Dudley, R. M. Central limit theorems for empirical measures. *The Annals of Probability*, pp. 899–929, 1978.

Gallier, J. H. and Quaintance, J. *Differential Geometry and Lie Groups: A Computational Perspective*, volume 12. Springer Nature, 2020.

Ganea, O.-E., Bécigneul, G., and Hofmann, T. Hyperbolic neural networks. *arXiv preprint arXiv:1805.09112*, 2018.

Gu, A., Sala, F., Gunel, B., and Ré, C. Learning mixed-curvature representations in product spaces. In *International Conference on Learning Representations*, 2018.

Khrulkov, V., Mirvakhabova, L., Ustinova, E., Oseledets, I., and Lempitsky, V. Hyperbolic image embeddings. In *Proceedings of the IEEE/CVF Conference on Computer Vision and Pattern Recognition*, pp. 6418–6428, 2020.

Lake, B. M., Salakhutdinov, R., and Tenenbaum, J. B. Human-level concept learning through probabilistic program induction. *Science*, 350(6266):1332–1338, 2015.

LeCun, Y., Bottou, L., Bengio, Y., and Haffner, P. Gradient-based learning applied to document recognition. *Proceedings of the IEEE*, 86(11):2278–2324, 1998.

Lee, J. M. *Riemannian manifolds: an introduction to curvature*, volume 176. Springer Science & Business Media, 2006.

Liu, Q., Nickel, M., and Kiela, D. Hyperbolic graph neural networks. In *Advances in Neural Information Processing Systems*, pp. 8230–8241, 2019.

Meng, Y., Huang, J., Wang, G., Zhang, C., Zhuang, H., Kaplan, L., and Han, J. Spherical text embedding. In *Advances in Neural Information Processing Systems*, pp. 8208–8217, 2019.

Nickel, M. and Kiela, D. Poincaré embeddings for learning hierarchical representations. In *Advances in neural information processing systems*, pp. 6338–6347, 2017.

Novikoff, A. B. On convergence proofs for perceptrons. Technical report, STANFORD RESEARCH INST MENLO PARK CA, 1963.

Platt, J. et al. Probabilistic outputs for support vector machines and comparisons to regularized likelihood methods. *Advances in large margin classifiers*, 10(3):61–74, 1999.

Ratcliffe, J. G., Axler, S., and Ribet, K. *Foundations of hyperbolic manifolds*, volume 149. Springer, 1994.

Sala, F., De Sa, C., Gu, A., and Ré, C. Representation tradeoffs for hyperbolic embeddings. In *International conference on machine learning*, pp. 4460–4469. PMLR, 2018.

Salakhutdinov, R. and Murray, I. On the quantitative analysis of deep belief networks. In *Proceedings of the 25th international conference on Machine learning*, pp. 872–879, 2008.

Shalev-Shwartz, S. and Ben-David, S. *Understanding machine learning: From theory to algorithms*. Cambridge university press, 2014.

Shimizu, R., Mukuta, Y., and Harada, T. Hyperbolic neural networks++. *arXiv preprint arXiv:2006.08210*, 2020.

Skopek, O., Ganea, O.-E., and Bécigneul, G. Mixed-curvature variational autoencoders. In *International Conference on Learning Representations*, 2020.

Steinwart, I. On the influence of the kernel on the consistency of support vector machines. *Journal of machine learning research*, 2(Nov):67–93, 2001.

Tabaghi, P. and Dokmanić, I. Geometry of comparisons. *arXiv preprint arXiv:2006.09858*, 2020a.

Tabaghi, P. and Dokmanić, I. Hyperbolic distance matrices.
In *Proceedings of the 26th ACM SIGKDD International Conference on Knowledge Discovery & Data Mining*, pp. 1728–1738, 2020b.

Tifrea, A., Bécigneul, G., and Ganea, O.-E. Poincaré GloVe: Hyperbolic word embeddings. *arXiv preprint arXiv:1810.06546*, 2018.

Tu, L. W. An introduction to manifolds. second, 2011.

Vapnik, V. *The nature of statistical learning theory*. Springer science & business media, 2013.

Weber, M., Zaheer, M., Rawat, A. S., Menon, A., and Kumar, S. Robust large-margin learning in hyperbolic space. *arXiv preprint arXiv:2004.05465*, 2020.

A. A Basic Review of Space Forms

Space forms are Riemannian manifolds of dimension $d \geq 2$ that are isomorphic to spherical, Euclidean or hyperbolic spaces (Lee, 2006). A d -dimensional spherical space with curvature $C > 0$ is a collection of points $\mathbb{S}_C^d = \{x \in \mathbb{R}^{d+1} : \langle x, x \rangle = C^{-1}\}$, where $\langle \cdot, \cdot \rangle$ is defined in the main text. Similarly, a d -dimensional hyperbolic space (i.e., the 'Loid model) with curvature $C < 0$ is a collection of points of the form $\mathbb{H}_C^d = \{x \in \mathbb{R}^{d+1} : [x, x] = C^{-1}\}$, where $[\cdot, \cdot]$ is defined in the main text. In Table 2, we list the Riemannian metric, exponential and logarithmic maps for each of these spaces. In sections B and C, we provide the proofs of Propositions 1 and 2 for space forms with arbitrary curvatures.

B. Proof of Proposition 1

Let $p \in \mathbb{S}_C^d$ and $w \in T_p \mathbb{S}_C^d = p^\perp$ such that $\langle w, w \rangle = C$. The separation surface $H_{p,w}$ is defined as

$$\begin{aligned} H_{p,w} &= \{x \in \mathbb{S}_C^d : g_p(\log_p(x), w) = 0\} \\ &= \{x \in \mathbb{S}_C^d : \langle x, w \rangle = 0\}. \end{aligned}$$

We can compute the distance between $x \in \mathbb{S}_C^d$ and $H_{p,w}$ as

$$d(x, H_{p,w}) = \min_{y \in H_{p,w}} \frac{1}{\sqrt{|C|}} \text{acos}(C y^\top x).$$

The projection of a point onto $H_{p,w}$ can be computed by solving the following constrained optimization problem

$$\max_{y \in \mathbb{R}^{d+1}} x^\top y \text{ such that } w^\top y = 0, \langle y, y \rangle = C^{-1}.$$

From the first order optimality condition for the Lagrangian, the projected point takes the form $\mathcal{P}(x) = \alpha x + \beta w$, where $\alpha, \beta \in \mathbb{R}$. Now, we impose the following subspace constraint,

$$\begin{aligned} w^\top \mathcal{P}(x) &= (\alpha x + \beta w)^\top w \\ &= \alpha x^\top w + \beta w^\top w \\ &= \alpha x^\top w + \beta C \\ &= 0, \end{aligned}$$

which gives $\beta = -\alpha C^{-1} x^\top w$. Subsequently, we have $\mathcal{P}(x) = \alpha(x - C^{-1} x^\top w w)$. On the other hand, from the norm constraint, we have

$$\begin{aligned} \|\mathcal{P}(x)\|^2 &= \alpha^2 (C^{-1} + C^{-1} (x^\top w)^2 - 2C^{-1} (x^\top w)^2) \\ &= \alpha^2 C^{-1} (1 - (x^\top w)^2) \\ &= C^{-1}, \end{aligned}$$

which gives $\alpha = (1 - (x^\top w)^2)^{-\frac{1}{2}}$.

Next, let us define $\psi = \text{acos}(x^\top w)$, where $\psi \in [0, \pi]$. Then,

$$\mathcal{P}(x) = \sqrt{\frac{1}{1 - \cos^2 \psi}} (x - C^{-1} \cos \psi w) = \frac{C^{-\frac{1}{2}}}{\|P_w^\perp x\|_2} P_w^\perp x, \quad (14)$$

Table 2. Summary of relevant operators in Euclidean, spherical, and hyperbolic ('Loid model) spaces with arbitrary curvatures.

\mathcal{M}	$T_p \mathcal{M}$	$g_p(u, v)$	$\log_p(x) : \theta = \sqrt{ C } d(x, p)$	$\exp_p(v)$	$d(x, p)$
\mathbb{R}^d	\mathbb{R}^d	$\langle u, v \rangle$	$x - p$	$p + v$	$\ x - p\ _2$
\mathbb{S}^d	p^\perp	$\langle u, v \rangle$	$\frac{\theta}{\sin(\theta)}(x - p \cos \theta)$	$\cos(\sqrt{ C } \ v\)p + \sin(\sqrt{ C } \ v\) \frac{v}{\sqrt{ C } \ v\ }$	$\frac{1}{\sqrt{ C }} \text{acos}(C \langle x, p \rangle)$
\mathbb{L}^d	p^\perp	$[u, v]$	$\frac{\theta}{\sinh(\theta)}(x - p \cosh \theta)$	$\cosh(\sqrt{- C } \ v\)p + \sinh(\sqrt{- C } \ v\) \frac{v}{\sqrt{- C } \ v\ }$	$\frac{1}{\sqrt{- C }} \text{acosh}(C [x, p])$

where $P_w^\perp x = x - \frac{1}{\langle w, w \rangle} \langle x, w \rangle w$. The minimum distance is given by

$$\begin{aligned}
 d(x, \mathcal{P}(x)) &= \frac{1}{\sqrt{C}} \text{acos}(Cx^\top \mathcal{P}(x)) \\
 &= \frac{1}{\sqrt{C}} \text{acos}\left(\sqrt{\frac{1}{1 - \cos^2 \psi}}(1 - \cos^2 \psi)\right) \\
 &= \frac{1}{\sqrt{C}} \text{acos}(|\sin \psi|) \\
 &\stackrel{(a)}{=} \frac{1}{\sqrt{C}} \text{asin}(|\cos \psi|) \\
 &= \frac{1}{\sqrt{C}} \text{asin}|x^\top w|,
 \end{aligned}$$

where (a) follows due to $\text{acos}(|\sin(\psi)|) = \text{asin}(|\cos(\psi)|)$, or

$$\begin{aligned}
 \cos(\text{asin}(|\cos \psi|)) &= \cos(\text{asin}\left(|\sin\left(\frac{\pi}{2} - \psi\right)|\right)) \\
 &= \cos\left(|\text{asin}(\sin(\frac{\pi}{2} - \psi))|\right) \\
 &= \cos\left(\left|\frac{\pi}{2} - \psi\right|\right) \\
 &= |\sin \psi|,
 \end{aligned}$$

for $\psi \in [0, \pi]$. Now, let $x \in \mathbb{S}_C^d$, and let $\mathcal{P}(x)$ be as given in (14). We readily have $\mathcal{P}(x) \perp w$. Therefore,

$$\begin{aligned}
 w^\top \log_{\mathcal{P}(x)}(x) &= \frac{\text{acos}(C\mathcal{P}(x)^\top x)}{\sin(\text{acos}(C\mathcal{P}(x)^\top x))} x^\top w \\
 &\stackrel{(a)}{=} \frac{\text{acos}(C\mathcal{P}(x)^\top x)}{|x^\top w|} x^\top w \\
 &= \text{asin}(|x^\top w|) \text{sgn}(x^\top w) \\
 &= \text{asin}(x^\top w) = \text{sgn}(x^\top w) \sqrt{C} d(x, \mathcal{P}(x)),
 \end{aligned}$$

where (a) follows from

$$\begin{aligned}
 \sin(\text{acos}(C\mathcal{P}(x)^\top x)) &= \sin(\text{acos}(\sqrt{1 - (x^\top w)^2})) \\
 &= \sin(\text{asin}(|x^\top w|)) \\
 &= |x^\top w|.
 \end{aligned}$$

This completes the proof.

C. Proof of Proposition 2

Let \mathbb{H}_C^d be the 'Loid model with curvature $C < 0$ (usually set to $C = -1$ for simplicity). The projection of $x \in \mathbb{H}_C^d$ onto $H_{p,w}$ is a point $\mathcal{P}(x) \in H_{p,w}$ that has the smallest distance to x . In other words, $\mathcal{P}(x)$ is the solution to the following constrained optimization problem

$$\max_y [y, x] \text{ such that } [y, y] = C^{-1}, [w, y] = 0,$$

where $[w, w] = -C$. This leads to $\mathcal{P}(x) = \alpha x + \beta w$, where $\alpha, \beta \in \mathbb{R}$. The subspace condition is enforced as follows:

$$\begin{aligned}
 [\mathcal{P}(x), w] &= \alpha[x, w] + \beta[w, w] \\
 &= \alpha[x, w] + \beta(-C) \\
 &= 0,
 \end{aligned}$$

which gives $\beta = \alpha C^{-1}[x, w]$, or $\mathcal{P}(x) = \alpha(x + C^{-1}[x, w]w)$. On the other hand, we also have

$$\begin{aligned} [\mathcal{P}(x), \mathcal{P}(x)] &= \alpha^2(C^{-1} - C^{-1}[x, w]^2 + 2C^{-1}[x, w]^2) \\ &= \alpha^2C^{-1}(1 + [x, w]^2) \\ &= C^{-1}. \end{aligned}$$

Then,

$$\mathcal{P}(x) = \sqrt{\frac{1}{1 + [x, w]^2}}(x + C^{-1}[x, w]w) = \frac{(-C)^{-\frac{1}{2}}}{\|P_w^\perp x\|} P_w^\perp x, \quad (15)$$

where $P_w^\perp x = x - \frac{1}{[x, w]}[x, w]w$ and $\|P_w^\perp x\| = \sqrt{-[P_w^\perp x, P_w^\perp x]}$. The minimum distance can be computed as

$$\begin{aligned} d(x, \mathcal{P}(x)) &= \frac{1}{\sqrt{-C}} \operatorname{acosh}(C[\mathcal{P}(x), x]) \\ &= \frac{1}{\sqrt{-C}} \operatorname{acosh}(C \sqrt{\frac{1}{1 + [x, w]^2}} C^{-1}(1 + [x, w]^2)) \\ &= \frac{1}{\sqrt{-C}} \operatorname{acosh}(\sqrt{1 + [x, w]^2}). \end{aligned}$$

We can further simplify this expression to¹:

$$d(x, \mathcal{P}(x)) = \frac{1}{\sqrt{-C}} \operatorname{asinh}([x, w]).$$

Now, let $x \in \mathbb{L}^d$ and let $\mathcal{P}(x)$ be given in (15). We can easily see that $[\mathcal{P}(x), w] = 0$. Therefore, we have

$$\begin{aligned} g_{\mathcal{P}(x)}(w, \log_{\mathcal{P}(x)}(x)) &= \frac{\operatorname{acosh}(C[\mathcal{P}(x), x])}{\sinh(\operatorname{acosh}(C[\mathcal{P}(x), x]))} [x, w] \\ &= \frac{\operatorname{asinh}([x, w])}{|[x, w]|} [x, w] \\ &= \operatorname{asinh}([x, w]) \operatorname{sgn}([x, w]) \\ &= \operatorname{asinh}([x, w]) = \operatorname{sgn}([x, w]) \sqrt{-C} d(x, \mathcal{P}(x)). \end{aligned}$$

This completes the proof.

D. Proof of Theorem 1

The Vapnik-Chervonenkis (VC) dimension (Vapnik, 2013) of a linear classifier is equal to the maximum size of a point set that a set of linear classifiers can *shatter*, i.e., completely partition into classes independent on how the point in the set are labelled. We establish the VC dimension for all three space forms $\mathcal{M} = \mathbb{R}^d, \mathbb{S}^d$, and \mathbb{L}^d (clearly, the VC dimension of Euclidean space forms is well-known, as described below).

The Vapnik-Chervonenkis (VC) dimension of affine classifiers in \mathbb{R}^d is $d + 1$ (see the treatment of VC dimensions of Dudley classes described in (Dudley, 1978)). Therefore, there exists a set of $d + 1$ points that affine classifiers in \mathbb{R}^d can shatter. Note again the distinction between affine and linear classifiers in Euclidean spaces.

Next, let $x_1, \dots, x_N \in \mathbb{S}^d$ be a set of point in spherical space \mathbb{S}^d , which can be shattered by linear classifiers. In other words, we have

$$y_n = \operatorname{sgn}(\operatorname{asin}(u_S^\top x_n)), \quad \forall n \in [N],$$

and for any set of binary labels $(y_n)_{n \in [N]}$. The linear classifiers in spherical space are a subset of linear classifiers in a $(d + 1)$ -dimensional Euclidean space. Hence, their VC dimension must be less than or equal to $d + 1$. On the other hand, if

¹Since $\cosh(x)^2 - \sinh(x)^2 = 1$.

we project a set of $d + 1$ points in \mathbb{R}^{d+1} , that can be shattered by linear classifiers in Euclidean space, onto \mathbb{S}^d (by a simple normalization), we can find a set of (exactly) $d + 1$ points that can be shattered by linear classifiers in \mathbb{S}^d . Hence, the VC dimension of linear classifiers in \mathbb{S}^d is exactly $d + 1$.

Next, let us turn our attention to d -dimensional hyperbolic spaces, namely the 'Loid model. Let $\mathcal{X} = \{x_n\}_{n \in [d+1]}$ be a set of $d + 1$ points in d -dimensional 'Loid model of hyperbolic space such that

$$x_n = \begin{bmatrix} \sqrt{1 + \|z_n\|^2} \\ z_n, \end{bmatrix}$$

for $z_n \in \mathbb{R}^d$ and all $n \in [d + 1]$. Furthermore, we assume that $z_1 = 0$, and $z_n = e_{n-1}$ for $n \in \{2, \dots, d + 1\}$, where e_n is the n -th standard basis vector of \mathbb{R}^d .

We claim that this point set can be shattered by the set of linear classifiers in hyperbolic spaces, i.e.,

$$l_w^{\mathbb{H}}(x) = \text{sgn}(\text{asinh}([w, x])) \quad (16)$$

where $w \in \{x \in \mathbb{R}^{d+1} : [x, x] > 0\}$. Let (y_1, \dots, y_{d+1}) be an arbitrary set of labels in $\{-1, 1\}$. Then, we define

$$t_1 = y_1, \quad t_n = ky_n, \quad \text{for } n \in \{2, \dots, d + 1\} \quad (17)$$

where $k > \sqrt{2} + 1$. Therefore, if we can show that there exists a $w \in \{x \in \mathbb{R}^{d+1} : [x, x] > 0\}$ such that

$$t_n = [w, x_n], \quad \forall n \in [d + 1],$$

then we have $y_n = l_w^{\mathbb{H}}(x_n)$ for all $n \in [d + 1]$. This is equivalent to showing that the following equation has a solution $w \in \{x : [x, x] > 0\}$,

$$t = X^{\top} H w,$$

where $t = (t_1, \dots, t_{d+1})$, and

$$X^{\top} = \begin{bmatrix} \sqrt{1 + \|z_1\|^2} & z_1^{\top} \\ \sqrt{1 + \|z_2\|^2} & z_2^{\top} \\ \vdots & \vdots \\ \sqrt{1 + \|z_{d+1}\|^2} & z_{d+1}^{\top} \end{bmatrix} = \begin{bmatrix} 1 & 0^{\top} \\ \sqrt{2} & e_1^{\top} \\ \vdots & \vdots \\ \sqrt{2} & e_d^{\top} \end{bmatrix}.$$

The solution is $w = H(X^{\top})^{-1}t$, described below,

$$w = H \begin{bmatrix} 1 & 0^{\top} \\ -\sqrt{2} & e_1^{\top} \\ \vdots & \vdots \\ -\sqrt{2} & e_d^{\top} \end{bmatrix} t = \begin{bmatrix} -t_1 \\ -\sqrt{2}t_1 + t_2 \\ \vdots \\ -\sqrt{2}t_1 + t_{d+1} \end{bmatrix}.$$

As the final step, we show that $w \in \{x : [x, x] > 0\}$. To this end we observe that

$$\begin{aligned} [w, w] &= -t_1^2 + \sum_{n=2}^{d+1} (-\sqrt{2}t_1 + t_n)^2 \\ &\stackrel{(a)}{=} y_1^2 \left(-1 + \sum_{n=2}^{d+1} (-\sqrt{2} + k \frac{y_n}{y_1})^2 \right) \\ &\stackrel{(b)}{=} -1 + \sum_{n=2}^{d+1} (-\sqrt{2} + k \frac{y_n}{y_1})^2 \\ &\stackrel{(c)}{>} 0, \end{aligned}$$

where (a) is due to (17), (b) follows from $y_n \in \{-1, 1\}$, and (c) is obvious if $k > \sqrt{2} + 1$. Therefore, linear hyperbolic classifiers can generate any set of labels for the point set $\{x_n\}_{n \in [d+1]}$. Furthermore, hyperbolic classifiers in (16) can be seen as linear classifiers in $d + 1$ dimensional Euclidean space. Hence, the VC dimension of linear classifiers in hyperbolic space is exactly $d + 1$.

From Theorem 1 and the fundamental theorem of concept learning (Shalev-Shwartz & Ben-David, 2014), the function class \mathcal{L} is probably accurately correctly (PAC) learnable. More precisely, let \mathcal{P} be a family of probability distributions on $\mathcal{M} \times \{-1, 1\}$, and let $\{(x_n, y_n)\}_{n \in [N]}$ be a set of i.i.d. samples from $P \in \mathcal{P}$. Then, we have

$$\inf_{l \in \mathcal{L}} P(\hat{l}_N(X) \neq Y) \leq \inf_{l \in \mathcal{L}} P(l(X) \neq Y) + C \sqrt{\frac{d+1}{n}} + \sqrt{\frac{2 \log(\frac{1}{\delta})}{n}}$$

where $\hat{l}_N = \arg \min_{l \in \mathcal{L}} \frac{1}{N} \sum_{n \in [N]} 1(l(x_n) \neq y_n)$ is the empirical risk minimizer. Therefore, all our classifiers have the same learning complexity.

E. Proof of Theorem 2

Lemma 1. *Let $K(x_1, x_2) = \text{asin}(x_1^\top x_2)$, where $x_1, x_2 \in B_0 = \{x \in \mathbb{R}^d : \|x\|_2 \leq 1\}$. Then, there exists a Hilbert space \mathcal{H}_0 , and a mapping $\phi_0 : B_0 \rightarrow \mathcal{H}_0$ such that*

$$K(x_1, x_2) = \langle \phi_0(x_1), \phi_0(x_2) \rangle_{\mathcal{H}_0},$$

where $\langle \cdot, \cdot \rangle_{\mathcal{H}_0}$ is the inner product on \mathcal{H}_0 . Moreover, we can construct a space $\mathcal{H}'_0 \supset \mathcal{H}_0$ such that indefinite inner products of the form $\langle \cdot, M_0 \cdot \rangle_{\mathcal{H}_0}$ are well-defined on \mathcal{H}'_0 . The indefinite operator $M_0 : \mathcal{H}'_0 \rightarrow \mathcal{H}'_0$ admits the following representation

$$K_H(x_1, x_2) = \text{asinh}(x_1^\top x_2) = \langle \phi_0(x_1), M_0 \phi_0(x_2) \rangle_{\mathcal{H}_0},$$

for all x_1, x_2 in a compact subset of \mathbb{R}^d , and it satisfies $M_0^\top M_0 = \text{Id}$, where Id denotes the identity operator.

Proof. The Taylor series expansion of asin can be used to establish that

$$\text{asin}(x_1^\top x_2) = \sum_{n=0}^{\infty} \frac{(2n)!}{2^{2n}(n!)^2(2n+1)} (x_1^\top x_2)^{2n+1}, \quad (18)$$

where $|x_1^\top x_2| \leq 1$. All the coefficients of this Taylor series are nonnegative. Hence, from Theorem 2.1 in (Steinwart, 2001), this is a valid positive-definite kernel. Therefore, there is a Hilbert space \mathcal{H}_0 endowed with an inner product $\langle \cdot, \cdot \rangle_{\mathcal{H}_0}$ such that

$$\text{asin}(x_1^\top x_2) = \langle \phi_0(x_1), \phi_0(x_2) \rangle_{\mathcal{H}_0},$$

for $x_1, x_2 \in B_0$ and vectors $\phi_0(x_1)$ and $\phi_0(x_2) \in \mathcal{H}_0$.

On the other hand, we have

$$\text{asinh}(x_1^\top x_2) = \sum_{n=0}^{\infty} (-1)^n \frac{(2n)!}{2^{2n}(n!)^2(2n+1)} (x_1^\top x_2)^{2n+1},$$

where $x_1, x_2 \in B \subseteq \mathbb{R}^d$ — a compact subset of \mathbb{R}^d . This Taylor series is the same as the one given in (18) except for the alternating signs of the coefficients. The analytical construction of the vector $\phi_0(x)$ in (Steinwart, 2001) gives a straightforward way to define an indefinite operator $M_0 : \mathcal{H}'_0 \rightarrow \mathcal{H}'_0$ such that $M_0^\top M_0 = \text{Id}$, and

$$\text{asinh}(x_1^\top x_2) = \langle \phi_0(x_1), M_0 \phi_0(x_2) \rangle_{\mathcal{H}'_0}.$$

Note that M_0 is a finite-dimensional diagonal matrix with elements ± 1 that represent the signs of the Taylor series coefficients.

The space \mathcal{H}'_0 contains \mathcal{H}_0 with the same definite inner product, i.e., if $\phi_0(x), \phi_0(y) \in \mathcal{H}'_0 \cap \mathcal{H}$, then $\langle \phi_0(x), \phi_0(y) \rangle_{\mathcal{H}_0} = \langle \phi_0(x), \phi_0(y) \rangle_{\mathcal{H}'_0}$. However, a point $\phi_0(x) \in \mathcal{H}'_0 \setminus \mathcal{H}_0$ may have an unbounded norm, i.e., $\langle \phi_0(x), \phi_0(x) \rangle_{\mathcal{H}'_0} = \infty$. Nevertheless, the indefinite inner products of the form $\langle \phi_0(x), M_0 \phi_0(x) \rangle_{\mathcal{H}'_0}$ are always well-defined so long as $x \in B$, a compact subset of \mathbb{R}^d . This is due to the fact that the convergence domain for the Taylor series of $\text{asinh}(\cdot)$ is any compact subset of \mathbb{R} . Hence, we can simply define $\mathcal{H}'_0 = \{\phi(x) : x \in B \subset \mathbb{R}^d\}$, where B is a compact subset of \mathbb{R}^d . \square

Let $\{x_1, \dots, x_N\}$ be a set of N points in the product space \mathcal{M} . For any point $x = [x_{\mathbb{E}}, x_{\mathbb{S}}, x_{\mathbb{H}}] \in \mathcal{M}$, we define

$$\phi(x) = (1, x_{\mathbb{E}}, C_{\mathbb{S}}^{-1/4} \phi_0(\sqrt{C_{\mathbb{S}}} x_{\mathbb{S}}), (-C_{\mathbb{H}})^{-1/4} \phi_0(\frac{1}{R_H} x_{\mathbb{H}})),$$

where $\phi(x)$ is defined as in the proof of Lemma 1, and R_H is an upper bound for the norm of the hyperbolic component of x , i.e., $\|x_H\|_2 \leq R_H$. Note that in order to distinguish the curvatures of different space forms, we added appropriate subscripts.

The linear classifier in product space form can be written as

$$\begin{aligned} l_w^{\mathcal{M}}(x) &= \operatorname{sgn}(w_E^T x_E + b + \frac{1}{\sqrt{C_{\mathbb{S}}}} \operatorname{asin}(w_S^T x_S) + \frac{1}{\sqrt{-C_{\mathbb{H}}}} \operatorname{asinh}((R_H H w_{\mathbb{H}})^T \frac{1}{R_H} x_{\mathbb{H}})) \\ &= \operatorname{sgn}(\langle w, M\phi(x) \rangle_{\mathcal{H}}), \end{aligned}$$

where \mathcal{H} is a simple product of $\mathbb{R}^{d_{\mathbb{E}}+1}$, \mathcal{H}_0 and \mathcal{H}'_0 accompanied by their corresponding inner products, $w = (b, w_E, C_{\mathbb{S}}^{-1/4} \phi_0(\frac{1}{\sqrt{C_{\mathbb{S}}}} w_{\mathbb{S}}), (-C_{\mathbb{H}})^{-1/4} \phi_0(R_H w_{\mathbb{H}})) \in \mathcal{H}$, and $M = \operatorname{diag}\{I, I, M_0\}$ is a product operator on \mathcal{H} such that

$$\langle w, M\phi(x) \rangle_{\mathcal{H}} = w_E^T x_E + b + \frac{1}{\sqrt{C_{\mathbb{S}}}} \langle \phi_0(\frac{1}{\sqrt{C_{\mathbb{S}}}} w_{\mathbb{S}}), \phi_0(\sqrt{C_{\mathbb{S}}} x_{\mathbb{S}}) \rangle_{\mathcal{H}_0} + \frac{1}{\sqrt{-C_{\mathbb{H}}}} \langle \phi_0(R_H H w_{\mathbb{H}}), M_0 \phi_0(\frac{1}{R_H} x_{\mathbb{H}}) \rangle_{\mathcal{H}'_0}.$$

From the problem assumptions, we assume the data points are linearly separable, i.e.,

$$y_n \langle w^*, M\phi(x_n) \rangle_{\mathcal{H}} \geq \gamma, \quad \forall n \in [N],$$

for a specific w^* in \mathcal{H} . Similar to the hyperbolic perceptron setting, we use the following update rule in RKHS

$$w^{k+1} = w^k + y_n M\phi(x_n) \text{ if } y_n \langle w^k, M\phi(x_n) \rangle_{\mathcal{H}} \leq 0.$$

If we initialize $w^0 = 0 \in \mathcal{H}$, we have

$$\begin{aligned} \langle w^*, w^{k+1} \rangle_{\mathcal{H}} &= \langle w^*, w^k \rangle_{\mathcal{H}} + \langle w^*, M y_n \phi(x_n) \rangle_{\mathcal{H}} \\ &\geq \langle w^*, w^k \rangle_{\mathcal{H}} + \gamma \\ &\geq k\gamma. \end{aligned}$$

On the other hand, we can bound the norm as

$$\begin{aligned} \langle w^{k+1}, w^{k+1} \rangle_{\mathcal{H}} &= \langle w^k, w^k \rangle_{\mathcal{H}} + \langle y_n M\phi(x_n), y_n M\phi(x_n) \rangle_{\mathcal{H}} + 2\langle w^k, y_n M\phi(x_n) \rangle_{\mathcal{H}} \\ &\leq \langle w^k, w^k \rangle_{\mathcal{H}} + \langle \phi(x_n), \phi(x_n) \rangle_{\mathcal{H}} \\ &\leq \langle w^k, w^k \rangle_{\mathcal{H}} + 1 + \|x_{n,\mathbb{E}}\|_2^2 + \frac{1}{\sqrt{C_{\mathbb{S}}}} \langle \phi_0(\sqrt{C_{\mathbb{S}}} x_{n,\mathbb{S}}), \phi_0(\sqrt{C_{\mathbb{S}}} x_{n,\mathbb{S}}) \rangle_{\mathcal{H}_0} + \frac{1}{\sqrt{-C_{\mathbb{H}}}} \langle \phi_0(\frac{1}{R_H} x_{n,\mathbb{H}}), \phi_0(\frac{1}{R_H} x_{n,\mathbb{H}}) \rangle_{\mathcal{H}'_0} \\ &\stackrel{(a)}{\leq} k(1 + R_E^2 + \pi), \end{aligned}$$

where R_E is an upper bound for the norm of the Euclidean components of the vectors, and (a) is due to

$$\langle \phi_0(\sqrt{C_{\mathbb{S}}} x_{n,\mathbb{S}}), \phi_0(\sqrt{C_{\mathbb{S}}} x_{n,\mathbb{S}}) \rangle_{\mathcal{H}_0} = \operatorname{asin}(C_{\mathbb{S}} x_{n,\mathbb{S}}^T x_{n,\mathbb{S}}) = \frac{\pi}{2},$$

and

$$\langle \phi_0(\frac{1}{R_H} x_{n,\mathbb{H}}), \phi_0(\frac{1}{R_H} x_{n,\mathbb{H}}) \rangle_{\mathcal{H}'_0} = \operatorname{asin}(\frac{1}{R_H^2} x_{n,\mathbb{H}}^T x_{n,\mathbb{H}}) \leq \frac{\pi}{2}.$$

Hence,

$$\begin{aligned} \frac{(\langle w^{k+1}, w^* \rangle_{\mathcal{H}})^2}{\langle w^{k+1}, w^{k+1} \rangle_{\mathcal{H}} \langle w^*, w^* \rangle_{\mathcal{H}}} &\geq \frac{k^2 \gamma^2}{k B_T \langle w^*, w^* \rangle_{\mathcal{H}}} \\ &= k \frac{\gamma^2}{B_T \langle w^*, w^* \rangle_{\mathcal{H}}}, \end{aligned}$$

where $B_T = 1 + R_E^2 + \frac{\pi}{2}(\frac{1}{\sqrt{C_{\mathbb{S}}}} + \frac{1}{\sqrt{-C_{\mathbb{H}}}})$. Therefore, convergence is guaranteed in $k \leq \frac{B_T \langle w^*, w^* \rangle_{\mathcal{H}}}{\gamma^2}$ steps. As a final remark, the upper bound for the ℓ_2 norm of $w_{\mathbb{H}}$ guarantees the boundedness of $\langle w^*, w^* \rangle_{\mathcal{H}}$.

F. Proof of Theorem 3

Let $w^0 = 0 \in \mathbb{R}^{d+1}$ and let $w^k \in \mathbb{R}^{d+1}$ be the estimated normal vector at the k -th iteration of the perceptron algorithm (see Algorithm 2). If the point $x_n \in \mathbb{L}^d$ ($y_n[w_k, x_n] < 0$) is missclassified, the perceptron algorithm produces the $(k+1)$ -th estimate of the normal vector according to

$$w^{k+1} = w^k + y_n H x_n.$$

Let w^* be the normal vector that classifies all the points with margin of at least γ , i.e., $y_n \operatorname{asinh}([w^*, x_n]) \geq \gamma, \forall n \in [N]$, and $[w^*, w^*] = 1$. Then, we have

$$\begin{aligned} (w^*)^\top w_{k+1} &= (w^*)^\top w^k + y_n [w^*, x_n] \\ &\geq (w^*)^\top w^k + \sinh(\gamma) \\ &\geq k \sinh(\gamma). \end{aligned}$$

In what follows, we provide an upper bound on $\|w^{k+1}\|^2$,

$$\begin{aligned} \|w_{k+1}\|^2 &= \|w^k + y_n H x_n\|^2 \\ &= \|w^k\|^2 + \|x_n\|^2 + 2y_n [w^k, x_n] \\ &\stackrel{(a)}{\leq} \|w^k\|^2 + R^2 \\ &= kR^2, \end{aligned}$$

where (a) is due to $\|x_n\|^2 \leq R^2$ and $y_n [w^k, x_n] \leq 0$, due to the error in classifying the point x_n . Hence,

$$\|w^{k+1}\| \leq \sqrt{k}R \text{ and } (w^*)^\top w^{k+1} \geq k \sinh(\gamma). \quad (19)$$

To complete the proof, define $\theta_k = \operatorname{acos}\left(\frac{(w^k)^\top w^*}{\|w^k\| \|w^*\|}\right)$. Then,

$$\begin{aligned} \frac{(w^{k+1})^\top w^*}{\|w^{k+1}\| \|w^*\|} &\stackrel{(a)}{\geq} \frac{k \sinh(\gamma)}{\sqrt{k}R \|w^*\|} \\ &= \sqrt{k} \frac{\sinh(\gamma)}{R \|w^*\|}, \end{aligned}$$

where (a) follows from (19). For $k \geq \left(\frac{R \|w^*\|}{\sinh(\gamma)}\right)^2$, we have $w^{k+1} = \alpha_{k+1} w^*$ for a positive scalar α_{k+1} . Hence, $\frac{1}{\sqrt{[w^{k+1}, w^{k+1}]}} w^{k+1} = w^*$.

G. Additional Experiments

We present additional experimental results not covered in the main text.

G.1. Convergence Analysis

As pointed out in Section 4.2, the hyperbolic perceptron described in (Weber et al., 2020) does not converge, which can be shown both through counterexamples and simulation studies. We report the following experimental results to validate this point and in particular, demonstrate that a convergence rate of $O\left(\frac{1}{\sinh(\varepsilon)}\right)$ is not possible.

First, we randomly generate a valid w^* such that $[w^*, w^*] = 1$. Then, we generate a random set of $N = 5,000$ points $\{x_i\}_{i=1}^N$ in \mathbb{L}^2 . For margin values $\varepsilon \in [0.1, 1]$, we remove points that violate the required distance to the classifier (parameterized with w^*), i.e., we decimate the points so that the condition $\forall n : |[w^*, x_n]| \geq \sinh(\varepsilon)$ is satisfied. Then, we assign binary labels to each data point according to the optimal classifier, so that $y_n = \operatorname{sgn}(\operatorname{asinh}([w^*, x_n]))$. We repeat this process for 100 different values of ε .

²Here, the norm is taken in the Euclidean sense, i.e., $\|w\| = \sqrt{w^\top w}$.

In the first experiment, we compare our proposed hyperbolic perceptron Algorithm 2 and the Algorithm 1 in (Weber et al., 2020) by running the methods until the number of updates achieved a predetermined upper bound (stated in Theorem 3) or until the classifier correctly classified all the data points. In Figure 6 (a), we report the classification accuracy of each method on the training data. Note that our theoretically established convergence rate $O\left(\frac{1}{\sinh^2(\varepsilon)}\right)$ is larger than $O\left(\frac{1}{\sinh(\varepsilon)}\right)$, the rate derived in Theorem 3.1 in (Weber et al., 2020). So, for the second experiment, we repeated the same process but terminate both algorithms after $O\left(\frac{1}{\sinh(\varepsilon)}\right)$ updates. The classification performance of the two algorithms under this setting is shown in Figure 6 (b). From these results, we can easily conclude that (1) our algorithm always converge within the theoretical upper bound provided in Theorem 3, and (2) both methods violate the theoretical convergence rate upper bound of (Weber et al., 2020).

G.2. Additional Results for Synthetic Data

We follow the same setup as described in Section 5 except that we now fix the optimal decision hyperplane w^* . Nine more experiments with different combinations of (N, ε) are shown in Figure 7. We observe that the number of updates made by the mixed-curvature perceptron is always smaller than the theoretical upper bound described in Theorem 2. And, in most cases, the mixed-curvature perceptron requires a smaller number of updates to converge than the Euclidean perceptron due to the fact that it accounts for the geometry of the data.

G.3. Discussion: Real-World Datasets

Following the procedure introduced in the work on mixed-curvature VAEs (Skopek et al., 2020), we embed the MNIST and Omniglot data sets into the product space $\mathbb{E}^2 \times \mathbb{S}^2 \times \mathbb{L}^2$. For MNIST, the curvature of the hyperbolic space is -0.129869 , and for the spherical space 0.286002 . For Omniglot, the curvature of the hyperbolic space is -0.173390 , and for the spherical space 0.214189 . Our experiments reveal that although the difference in the log-likelihood metric used to measure the quality of the mixed-curvature VAE and the Euclidean embedding is very small (see the results reported in (Skopek et al., 2020) and reproduced in Table 3), the performance gain of the mixed-curvature perceptron compared to the Euclidean perceptron can be as high as 9.56% for MNIST and 32.63% for Omniglot. This shows that the proposed mixed-curvature perceptron algorithm can indeed make better use of the features from a mixed-curvature spaces to perform the learning task.

Table 3. Estimated marginal log-likelihood after embedding the data into lower-dimensional spaces.

	MNIST	Omniglot
\mathbb{E}^6	-96.88 ± 0.16	-136.05 ± 0.29
$\mathbb{E}^2 \times \mathbb{S}^2 \times \mathbb{H}^2_{C_H}$	-96.71 ± 0.19	-135.93 ± 0.48

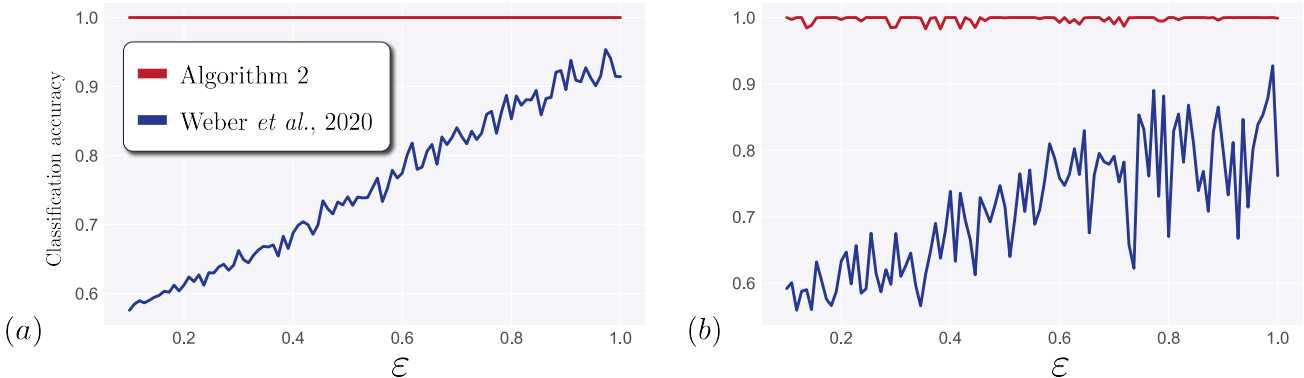


Figure 6. A comparison between the classification accuracy of our hyperbolic perceptron Algorithm 2 and the algorithm in (Weber et al., 2020) for different values of the margin ε . The classification accuracy is the average of five independent random trials. The stopping criterion is either a 100% classification accuracy or the theoretical upper bound in Theorem 3 (Figure (a)), and Theorem 3.1 in (Weber et al., 2020) (Figure (b)).

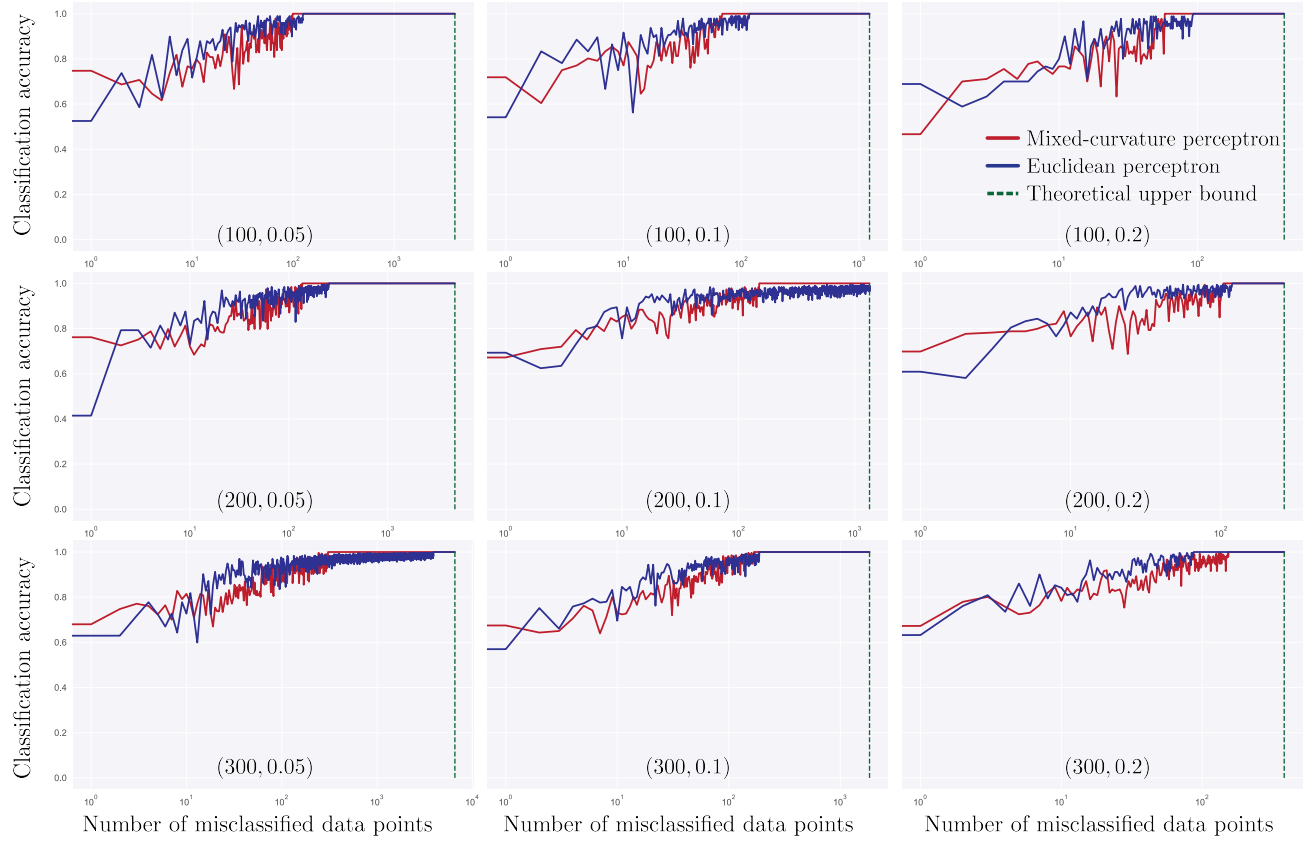


Figure 7. Classification accuracy after each update of the mixed-curvature and Euclidean perceptron algorithms for nine different combinations of (N, ε) .